Evidence of quadratic time dependence of the kinetics in a continuous order-disorder transition

Sabyasachi Karmakar,[1,2] Mrinmay K. Mukhopadhyay,[1,2,*] Milan K. Sanyal,[1,†] Alexander Meinhardt,[3,4] and Thomas F. Keller[3,4]

[1]*Saha Institute of Nuclear Physics, 1/AF Bidhannagar, Kolkata 700064, India*

[2]*Homi Bhabha National Institute, BARC Training School Complex, Anushaktinagar, Mumbai 400094, India*

[3]*Centre for X-ray and Nano Science CXNS, Deutsches Elektronen-Synchrotron(DESY), 22607 Hamburg, Germany*

[4]*Department of Physics University of Hamburg, Notkestraβe 9-11, 22607 Hamburg, Germany*

(Received 23 July 2024; revised 19 November 2024; accepted 23 December 2024; published 10 January 2025)

Kinetics of order-disorder transitions including melting in low-dimensional systems is theoretically predicted to be heterogeneous that start by nucleation in defect sites at lower than homogeneous bulk-melting temperature requiring substantially lower energy barrier. We probed kinetics of such transition in thin multilayered films using x-ray scattering and *in situ* atomic force microscopy (AFM) studies. X-ray results show linear increase with time in in-plane separation of ordered domains while *in situ* AFM measurements show a linear increase in height of disordered domains with time. The structure factor of the diffraction peak reduces linearly with square of time as the material disorder.

DOI: 10.1103/PhysRevB.111.024105

I. INTRODUCTION

The emergence of several novel two-dimensional (2D) materials since the discovery of graphene has rejuvenated the interest in order-disorder phase-transitions including melting and thermal properties of ultrathin films [1]. Implications of the reduced dimensionality in order-disorder transitions were always important to understand the fundamental physics [2] and now, the applications of various 2D materials in several technological areas from electronics, and photonics to phononics, have made thermal management an essential topic. In a first-order phase transition in 3D materials, the required latent heat originates from a discontinuous entropy change. Since entropy is an extensive quantity, the volume reduction resulting from the dimensionality change can significantly lower the latent heat. As a result, compared to 3D materials, 2D materials typically require much less energy to initiate a readable phase change and even the topological defects can mediate phase transitions in 2D materials [3]. The defects of materials such as point defects, stacking faults, or grain boundaries act as the nucleation point for such phase transitions in 2D materials. In all these cases, the melting transitions can be continuous in nature, making it difficult to define a melting point. Additionally, the transition temperature can depend on the heating rate as predicted in theory and also observed experimentally [3,4].

Thermodynamic definition of the melting temperature T_m suggests the coexistence of the ordered-solid and liquid phases as Gibbs free energies of the two phases are equal, and above T_m the solid is unstable and as a result, homogeneous melting occurs. However, heterogeneous melting is found at lower than T_m in materials with significant defects originating from the defect sites [5,6]. It is also established that other types of phase transitions in materials that destroy long-range order such as an order-disorder transition in multilayered structures, solid-state amorphization initiated by external perturbations like heat, laser excitation, or by ion irradiation, proceed by the same two distinct mechanisms as homogeneous and heterogeneous melting [7]. Theoretical and simulation studies have shown that the kinetics of such phase transitions differ from conventional homogeneous transitions requiring substantially lower temperature and latent heat. Ultrafast electron diffraction studies on both the single crystalline and polycrystalline gold thin films show the presence of three distinct melting regimes—homogeneous, heterogeneous, and incomplete, depending on the adsorbed energy densities [7]. Time-resolved x-ray diffraction study on the melting of a polycrystalline gold thin film using pulsed-laser heating shows the formation of a melting band that originates at the grain boundaries and propagates into the grains [8]. It was observed that the integrated intensity of Bragg peaks decays exponentially with time and that depends on film thicknesses and laser fluence. The study of the kinetics of melting transitions presents interesting physics and is also crucial for identifying properties like critical temperature, thermal stability, etc. Despite all these studies, kinematical visualization of phase transitions in 2D materials and corresponding physical properties has remained enigmatic requiring more attention. Most of the studies performed in this direction are on either monoatomic or diatomic systems and provide insight into atomic scale but the polyatomic organometallic systems are yet to be explored and that may lead to different scenarios as the molecular migration is expected to be sluggish in the transition.

Organic molecules with a π-conjugated system like metal-phthalocyanines (MPcs) crystallize in phases and display

*Contact author: mrinmay.mukhopadhyay@saha.ac.in

†Contact author: milank.sanyal@saha.ac.in

semiconducting character. MPcs have been widely explored for fabricating electronic devices such as organic light-emitting diodes (OLED), field effect transistors, solar cells, sensors, and spintronic devices like spin valves, magnetic sensors, and spin OLEDs [9–11]. The performance of these devices is greatly affected due to high working temperature or heating related to high current flow [12,13]. Although it is clear that higher temperature has a deleterious effect on device performance, temperature-dependent physical properties of the organometallic materials remains partially unclear. Copper-phthalocyanine (CuPc) is one of the very important members of the MPc family and is well known for its structural simplicity, chemical, and thermal stability. CuPc thin-film forms well defined columnlike structures over the substrate [14]. A very thin homogeneous film of CuPc can be considered equivalent to a quasi-two-dimensional system and a potential model system for studying the phase transition in organic small molecular semiconductors. However, the molecules involved in these cases are very large compared to the inorganic systems. So, the molecular migration will take a much longer time than monoatomic molecules. On the other hand, the application of very high temperatures can cause direct evaporation of the film or may result in dissociation of the organic molecules. So, to study the kinetics of phase transition using conventional x-ray scattering techniques in these systems, we carried out the measurements at a relatively lower temperature and for a longer time scale.

We have prepared copper-phthalocyanine (CuPc) thin films and studied the kinetics of this transition at an elevated temperature (∼250 °C, much below the melting temperature of the bulk CuPc, 350 °C) as a function of time using x-ray scattering and AFM studies. We found that the order-disorder transition is continuous in nature and it initiates from the defect sites of ordered domain grain boundaries. Both the in-plane and out-of-plane electron densities were found to be linearly decaying with time leading to a quadratic-time dependence of structure factor decay of the multilayer Bragg peak in the process of evolution of the disordered structures within the material and the rate of the decay scales with the thickness of the film through an exponent.

II. EXPERIMENTAL DETAILS

CuPc films have been deposited following the procedure explained in our previous work [14]. The *ex situ* x-ray reflectivity (XRR) measurements were performed at 1.54 Å wavelength using a Rigaku Smart Lab instrument while the *in situ* XRR and GISAXS were performed in the Indian Beamline at Photon Factory (BL-18B), KEK, Japan, with an incident beam of energy 12 keV. A Pilatus 1M detector was used for the GISAXS measurement in the beamline. All the *in situ* x-ray scattering studies were performed under an inert atmosphere using the DHS 1100 sample stage and the time-dependent order-disorder transition data on CuPc thin films were collected by maintaining a constant temperature of 250 °C in the sample stage. The *in situ* AFM topographic and phase images were collected at 250 °C temperature in constant dry nitrogen flow with a Bruker Nano Dimension Icon AFM instrument in tapping mode [15].

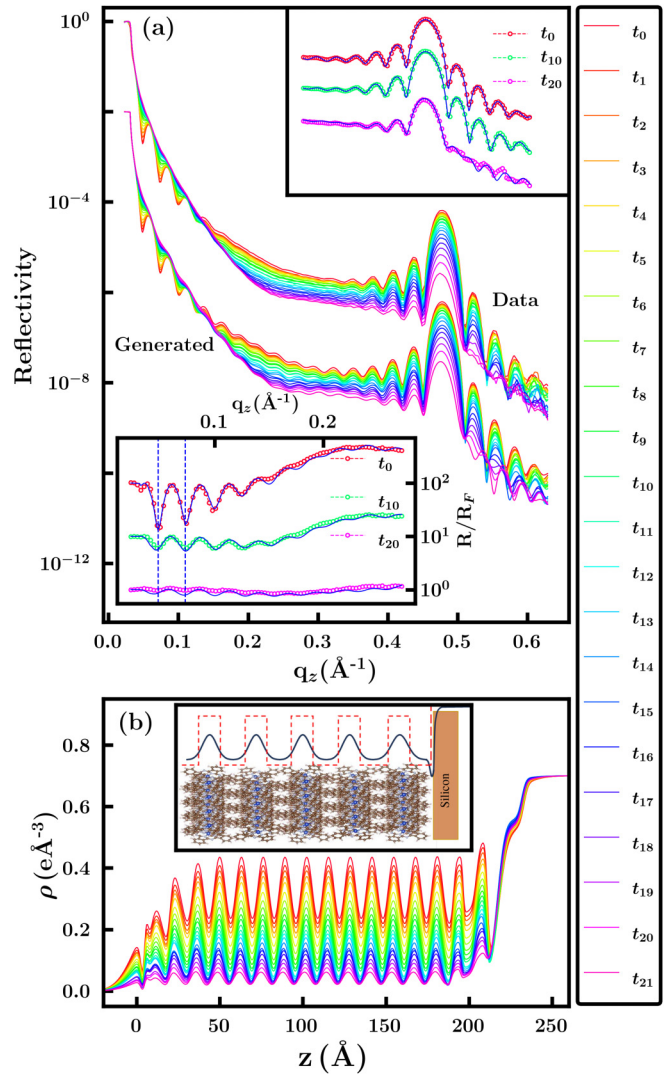

FIG. 1. (a) Experimental and calculated XRR profiles of CuPc film at 250 °C temperature as a function of time. Kiessig oscillations and the Bragg peak part of the XRR at three different times are shown on the upper and lower inset, respectively, to indicate the goodness of fit. Experimental data are open circles and blue lines are the fitted curves in the insets. (b) Corresponding EDP profiles extracted from the fitting of XRR at different times are shown. The inset shows a schematic diagram of the molecular arrangement on the substrate and the associated electron density profile with this arrangement.

III. RESULTS AND DISCUSSION

XRR is a well-known nondestructive technique that gives the electron density profile (EDP) along the film thickness (out-of-plane direction), and the roughness in different layers of the materials in the film [14,16]. Figure 1(a) represents the time evolution of the XRR profile and corresponding fitted curves of one such film having thickness 221 Å. Here, t_i corresponds to the start time of an XRR measurement and the difference between two consecutive reflectivity profiles, i.e., $(t_{i+1} - t_i)$ is 10 min. The presence of a central Bragg peak and corresponding Laue oscillations are signatures of a homogeneous film, with coherent out-of-plane ordering and smooth interfaces [14,17,18]. We have used Parratt

formalism to fit the XRR profiles [16,19]. The extracted EDPs are shown in Fig. 1(b). We have modeled the film with multiple stacks of bilayers and each of the bilayers consists of a high-density and low-density regions of molecular arrangement on the substrate as shown in the schematic of the inset of Fig. 1(b). The red dashed line and the blue line correspond to EDP without roughness and with roughness convolution, respectively. In the insets of Fig. 1(a), three XRR profiles (t_0, t_{10}, and t_{20}) for two different regions in the q_z space, the Kiessig oscillations region (lower inset) and the Bragg peak-Laue oscillation region (upper inset), are shown superimposed over the corresponding fitted curves. This gives a clear view of the agreement between data and fit and confirms that the presented EDP model correctly represents the film structure along the out-of-plane direction. The Bragg peak and Laue oscillations can also be analyzed using different x-ray thin film refinement methods based on the Laue interference function [20–22]. But we can see that our EDP model based on Parratt formalism is capable of generating a sufficiently good fit for the whole q_z range of the data. The R/R_f plot, where R_f is the reflectivity from the substrate, the lower inset of Fig. 1(a) shows a decay of the Kiessig oscillation amplitudes with respect to time but the position of each oscillation remains unchanged as marked by the dotted line. The EDP profiles show a constant decrease in average electron density with increasing time. This indicates the formation of more and more defects within the film as the time of measurement increases at a high temperature. The specular reflection contribution in the total scattering from the well-ordered structure decreases resulting in a decrease in average electron density contribution to the reflectivity. As a result of this density inhomogeneity, the film became rough and the Kiessig oscillations also got smeared out. In the case of Bragg peak and Laue oscillations, we observe the same scenario, i.e., the peak intensity is decreasing continuously but the positions remain the same throughout the process. This result indicates that the number of out-of-plane ordered columns is decreasing with time due to the transformation to a disordered phase. This transition process is slow, and in an instant, the ordered columns that have not yet transformed to the disordered phase of the transition process keep their out-of-plane structure intact.

In order to get an idea about the nature of this transition and its dependency on temperature, we performed the same experiments at two different temperatures (240 °C and 260 °C) with two samples deposited in identical conditions. Here, the square root of the normalized intensity, defined as A, is calculated as a function of q_z and the value of A at the Bragg peak (A_p) which is proportional to the structure factor of the multilayer structure, has been plotted as a function of the square of the measurement time t in Fig. 2(a). In the inset, we have shown the calculated A from the measured intensity at four different times of measurements at 250 °C. The four circles in the middle curve represent the corresponding peak value of the four curves in the inset. From the line fits (red dashed line) on all three curves we can see that each of them follows a similar trend and A_p shows a linear dependence of t^2. In Fig. 2(b) we have plotted A_p vs t^2 for four samples with different thickness but kept at the same temperature (250 °C). All the curves can be fitted with a straight line having different slopes. To find the dependency with the thickness of the film,

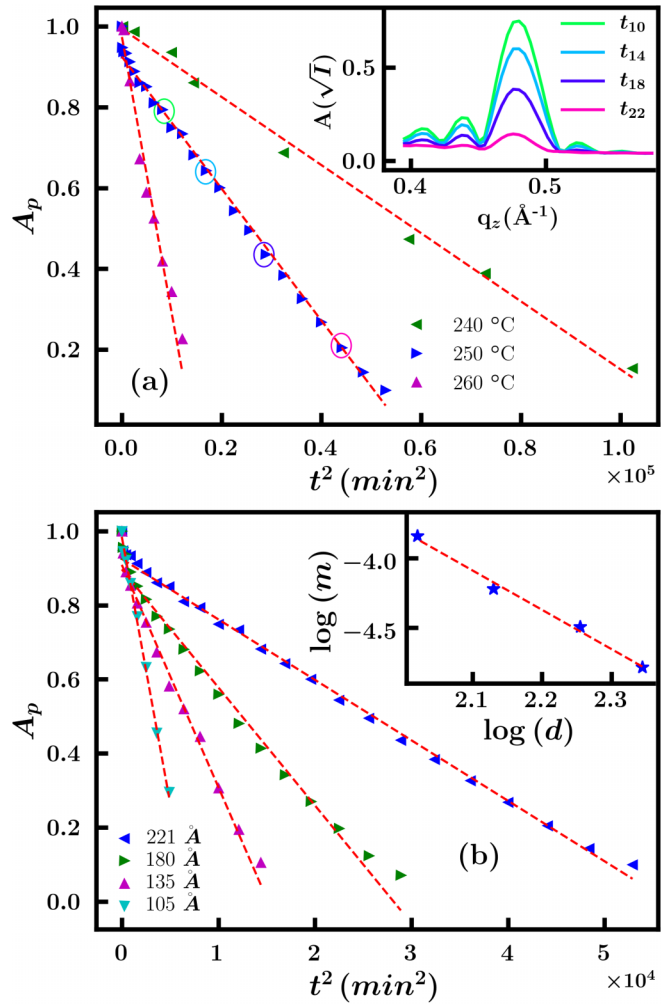

FIG. 2. (a) A_p vs t^2 plot for different temperature, where A is square root of the normalized intensity ($\sqrt{I}$) and A_p is the value of A at the Bragg peak position. Inset shows A vs q_z plot at four different times as marked by the circles in the A_p vs t^2 plot. (b) A_p vs t^2 plot for different thicknesses is shown, symbols represent the data and lines represent linear fit. Inset shows a log-log plot of different slopes of the line A_p vs t^2 fit as a function of thickness, line is the fit.

we have plotted each slope (m) from the linear fits of Fig. 2(b) with the corresponding thicknesses (d) in log-log scale, and the result is presented in the inset of Fig. 2(b). This linear dependence with a slope of $\nu = -2.83$ suggests the exponent nature of the slope with the film thickness d, as $m \propto d^{\nu}$.

We have also performed *in situ* GISAXS measurements to get an idea about the change in the in-plane ordering. The images taken at four different times of this order-disorder transition process are presented in Fig. 3(a). The first image shows a strong peak at $q_y = 0$ and a pair of in-plane correlation peaks on each side of the main peak [14]. These satellite peaks signify the presence of a 2D correlated in-plane structure. The line profiles, extracted from all the images are shown in Fig. 3(b) [the change in color from blue to red represents increasing time]. The in-plane correlation peaks change their shapes and become indistinguishable as the time of this transition process increases and ultimately end up in a disordered structure that corresponds to a small hump

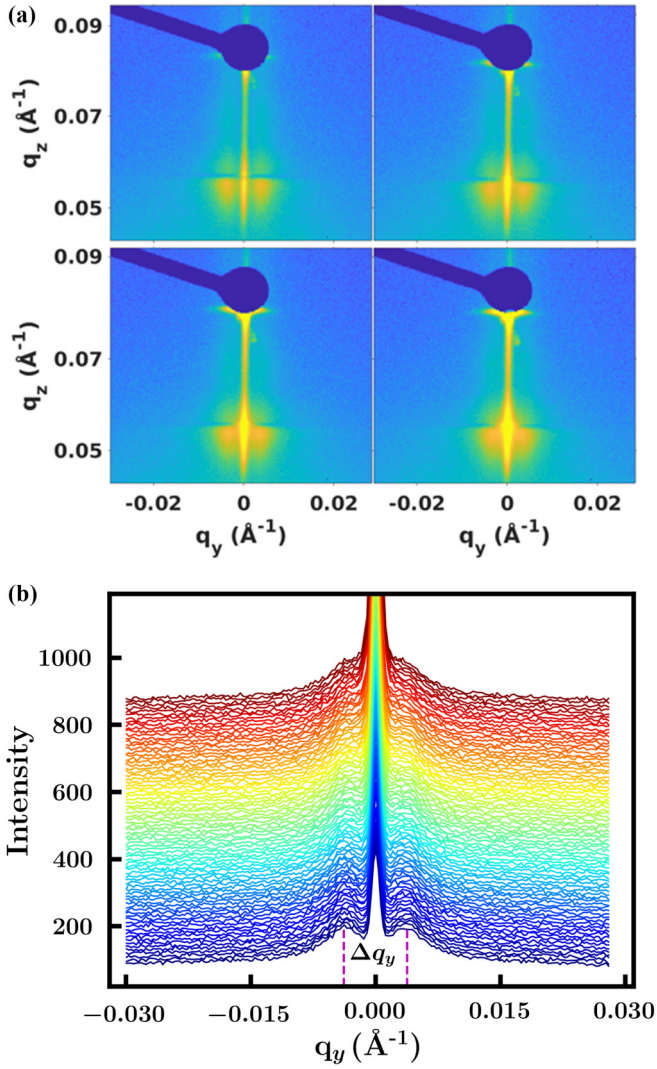

FIG. 3. (a) GISAXS image collected in a 2D detector at four different times during this order-disorder transition process. (b) Line profiles of all the images collected during time evolution. The curves are shifted vertically for better clarity. Amplitude ratios of the central peak at $q_y = 0$ and the corresponding side peak with respect to time are plotted in (c), and the line is the guide to the eye. Inset shows the variations in Δq_y with respect to time.

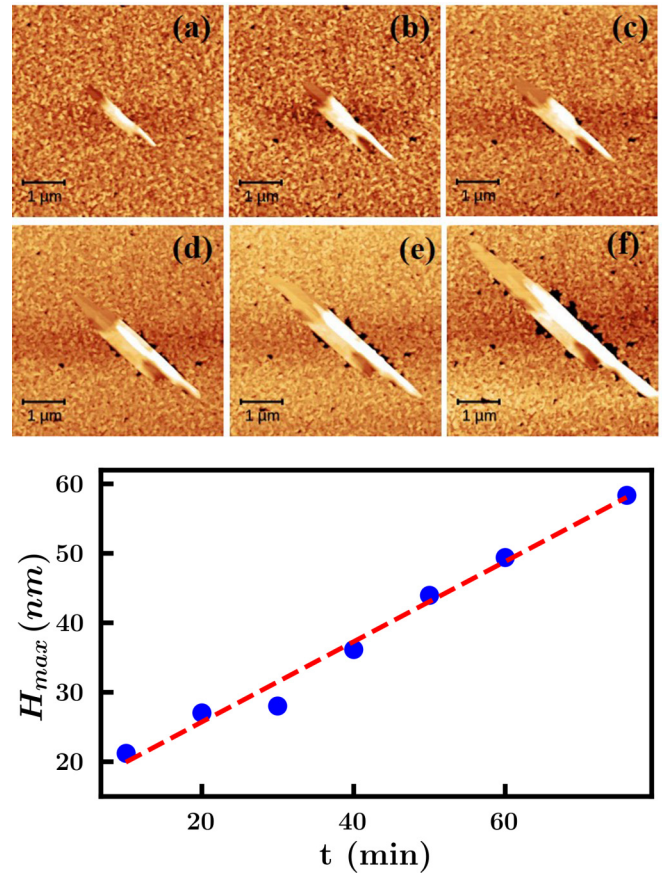

FIG. 4. (a)–(f) AFM topographic images acquired *in situ* at 250 °C during time evolution of the nucleated structure. The times(t) for the images from (a)–(f) are 10, 30, 40, 50, 60, and 76 min, respectively. (g) $H_{\max} - t$ plot, where $H_{\max}$ is the maximum height of the nucleated region.

at either side of the main peak. We have fitted all the profiles with three Lorentzian profiles and then extracted the ratio of amplitudes (A_r) between a side peak and the central peak. In Fig. 3(c) we have plotted the time dependence of A_r and it shows that this ratio is decreasing over time. The difference between the positions of the two side peaks (Δq_y) is plotted with time in Fig. 3(c) [inset] and it is found to be also decreasing with time. These observations indicate that the in-plane diffusion of molecular stacks causes the stack separation to increase linearly with time during this transition process. As a result of this diffusion of molecular stacks with time, the disordered phase increases, and the in-plane ordering decreases significantly.

In order to find a real-space picture of the transition and molecular propagation process, we have performed an *in situ* AFM experiment by heating the sample at 250 °C at an N_2 gas environment. The AFM images taken at six different times of this process are presented in Figs. 4(a)–4(f). First, we started with an overview scan of a large area (20 µm × 20 µm) and detected a nucleation site. Then, we focused on the nucleation site and started scanning over a small area (5 µm × 5 µm) to get a detailed image of the nucleating site. It is clear from

these topography images that the size of the nucleation site is increasing with time and also the void spots are appearing over a significant portion of the film. These images confirm that the molecular movement toward the defect sites is in accordance with the out-of-plane and in-plane movement of the molecular stack observed in x-ray scattering studies. The molecules migrate toward the nucleation sites and form a larger disordered structure as observed in the AFM image sequence. We have calculated the height of this nucleating structure and plotted it with time (t) in Fig. 4(g). The plot shows that the height of the nucleating object is linearly increasing with time. The amount of excess materials created due to increasing molecular-stack separation as observed in GISAXS measurement forms these molds at the nucleation sites.

The XRR studies of the time evolution of the order-disorder transition process in CuPc thin films reveal very little change in thickness of the film but the average electron density of the film decreases significantly with time. It also shows that the high-low alternate electron density structure almost remains intact [as shown in Fig. 1(b)] over the whole period of the transition process and only a few multilayer structures near the surface is getting modified with time. The decrease in average electron density was attributed to the decrease in contribution in the specular direction from the ordered multilayer stack due to the time evolution of disordered structures in the film. To parametrize the time evolution process of this transition, we have considered the EDP of the region from 100 Å to 155 Å of the film thickness [as shown in Fig. 5(a)] and calculated the average electron density difference ($\Delta\rho$) between the peak and the trough of the EDP. This $\Delta\rho$ has been plotted with the square of the evolution time t which can be fitted with a straight line as shown in Fig. 5(b). The change in $\Delta\rho$ is the result of migration of molecules from the melted molecular stack which has been shown in the model in Fig. 6. The GISAXS results show the linear dependence of the change in the in-plane separation of the ordered molecular stack with time and the *in situ* AFM images show linear increase in the height of the disordered structure with time. So the change in $\Delta\rho$, a signature of volumetric change in the structure, will change as t^2 as found in Fig. 5(b).

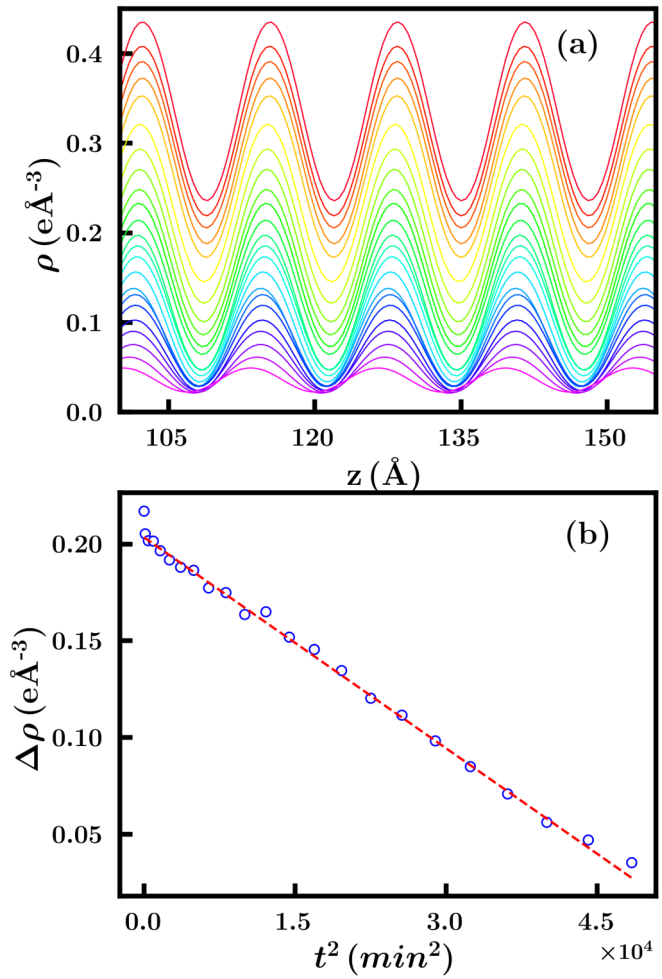

FIG. 5. (a) Magnified view of a portion of the EDP. (b) $\Delta\rho$ vs t^2 plot.

IV. CONCLUSION

We have probed the kinetics of the order-disorder transition of multilayered thin films using x-ray scattering and AFM studies. The thermally activated diffusion of molecules in both the in-plane and out-of-plane directions causes the breakdown of the ordered multilayer structure to the disordered structures. We have observed a t^2 decay of the structure factor of the multilayer Bragg peak as the ordered-to-disorder phase transition evolves and the rate of decay increases with an increase in temperature. The decay constant of the structure factor was also found to scale with the film thickness. The linear dependence of in-plane separation of the multilayer stack and the increase in height of the defect sites with time justifies the observation of the t^2 dependence of $\Delta\rho$ extracted from the EDP of the XRR profiles. This type of time dependence of the intensity decay during phase transition is different from the Arrhenius-type exponential decay which is observed during the melting transition of gold films [7,8]. The highly packed columnar nature of the film due to its intermolecular interaction and also the substrate-molecule interaction may impose constraints over the random motion of the molecular stacks. The experiment was performed in a relatively low and constant temperature which helped us to get precise control over the amount of supplied thermal energy and it decreased the chance of catastrophic collapse of the thin-film structure. This kind of imposed confinement makes the molecular stacks

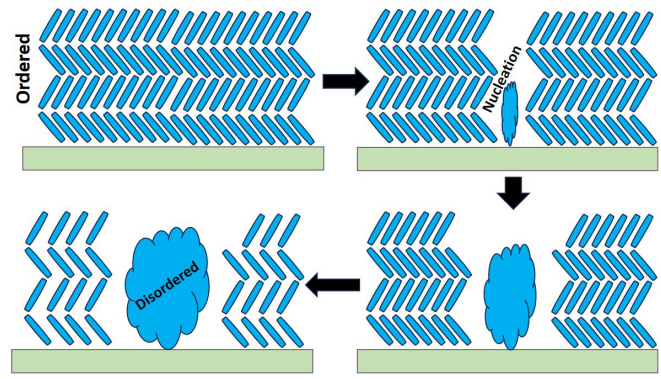

FIG. 6. Schematic representation of the order-disorder transition.

that are nearer to a defect region more vulnerable than the others and leads to a systematic collapse of the ordered structure. However, further detailed theoretical and experimental studies are needed to fully understand the origin and nature of this kind of time dependence. The exponent type dependence of the decay rate with the film thickness is also very crucial and may be useful to device applications and also to determine the working temperatures of the devices. We believe the experimental observation of such kinetic evolution shall promote further theoretical investigation of the heterogeneous phase transitions in technologically important low-dimensional materials.

ACKNOWLEDGMENTS

The authors acknowledge Mr. Arno Jeromin for AFM measurement. The authors also acknowledge the Department of Science and Technology, India, for the financial support and Jawaharlal Nehru Centre for Advanced Scientific Research, Bangalore, India, for facilitating the experiments at the Indian Beamline, Photon Factory, KEK, Japan. S.K. also acknowledges university grant commission (UGC) for providing financial assistance. M.K.S. acknowledges the support of the Indian National Science Academy Senior Scientist Programme.

[1] W. Li, X. Qian, and J. Li, Phase transitions in 2D materials, Nat. Rev. Mater. **6**, 829 (2021).

[2] K. J. Strandburg, Two-dimensional melting, Rev. Mod. Phys. **60**, 161 (1988).

[3] S. E. Nagler, P. M. Horn, T. F. Rosenbaum, R. J. Birgeneau, M. Sutton, S. G. J. Mochrie, D. E. Moncton, and R. Clarke, Orientational order in xenon fluid monolayers on single crystals of exfoliated graphite, Phys. Rev. B **32**, 7373 (1985).

[4] M. K. Mukhopadhyay, M. K. Sanyal, A. Datta, M. Mukherjee, T. Geue, J. Grenzer, and U. Pietsch, Transition from two-dimensional to three-dimensional melting in Langmuir-Blodgett films, Phys. Rev. B **70**, 245408 (2004).

[5] J. Berry, K. R. Elder, and M. Grant, Melting at dislocations and grain boundaries: A phase field crystal study, Phys. Rev. B **77**, 224114 (2008).

[6] S. R. Phillpot, S. Yip, and D. Wolf, How Do Crystals Melt?: Computer simulations demonstrate the interplay between thermodynamics and kinetics during the melting process, Comput. Phys. **3**, 20 (1989).

[7] M. Mo, Z. Chen, R. Li, M. Dunning, B. Witte, J. Baldwin, L. Fletcher, J. Kim, A. Ng, R. Redmer *et al.*, Heterogeneous to homogeneous melting transition visualized with ultrafast electron diffraction, Science **360**, 1451 (2018).

[8] T. A. Assefa, Y. Cao, S. Banerjee, S. Kim, D. Kim, H. Lee, S. Kim, J. H. Lee, S.-Y. Park, I. Eom *et al.*, Ultrafast x-ray diffraction study of melt-front dynamics in polycrystalline thin films, Sci. Adv. **6**, eaax2445 (2020).

[9] A. Babel, J. Wind, and S. Jenekhe, Ambipolar charge transport in air-stable polymer blend thin-film transistors, Adv. Funct. Mater. **14**, 891 (2004).

[10] A. Atxabal, M. Ribeiro, S. Parui, L. Urreta, E. Sagasta, X. Sun, R. Llopis, F. Casanova, and L. Hueso, Spin doping using transition metal phthalocyanine molecules, Nat. Commun. **7**, 13751 (2016).

[11] M. Warner, S. Din, I. S. Tupitsyn, G. W. Morley, A. M. Stoneham, J. A. Gardener, Z. Wu, A. J. Fisher, S. Heutz, C. W. Kay *et al.*, Potential for spin-based information processing in a thin-film molecular semiconductor, Nature (London) **503**, 504 (2013).

[12] S. Schuller, P. Schilinsky, J. Hauch, and C. Brabec, Determination of the degradation constant of bulk heterojunction solar cells by accelerated lifetime measurements, Appl. Phys. A **79**, 37 (2004).

[13] A. Sassella, D. Braga, M. Campione, T. Ciabattoni, M. Moret, J. Parravicini, and G. Parravicini, Probing phase transitions and stability of organic semiconductor single crystals by dielectric investigation, J. Appl. Phys. **109**, 013529 (2011).

[14] S. Karmakar, M. K. Mukhopadhyay, and M. K. Sanyal, Investigation of the structure-transport correlation in metal phthalocyanine thin films, Phys. Rev. Mater. **8**, 024601 (2024).

[15] A. Stierle, T. F. Keller, H. Noei, V. Vonk, and R. Roehlsberger, DESY NanoLab, J. Large-Scale Res. Facil. **2**, A76 (2016).

[16] M. K. Sanyal, M. K. Mukhopadhyay, M. Mukherjee, A. Datta, J. K. Basu, and J. Penfold, Role of molecular self-assembling in Langmuir-Blodgett film growth, Phys. Rev. B **65**, 033409 (2002).

[17] A. C. Dürr, F. Schreiber, M. Münch, N. Karl, B. Krause, V. Kruppa, and H. Dosch, High structural order in thin films of the organic semiconductor diindenoperylene, Appl. Phys. Lett. **81**, 2276 (2002).

[18] C. Ern, W. Donner, H. Dosch, B. Adams, and D. Nowikow, Temperature-dependent interfacial stiffness of the disorder layer in a thin Cu_3Au alloy film, Phys. Rev. Lett. **85**, 1926 (2000).

[19] L. G. Parratt, Surface studies of solids by total reflection of x-rays, Phys. Rev. **95**, 359 (1954).

[20] C. W. Miller, A. Sharoni, G. Liu, C. N. Colesniuc, B. Fruhberger, and I. K. Schuller, Quantitative structural analysis of organic thin films: An x-ray diffraction study, Phys. Rev. B **72**, 104113 (2005).

[21] E. E. Fullerton, I. K. Schuller, H. Vanderstraeten, and Y. Bruynseraede, Structural refinement of superlattices from x-ray diffraction, Phys. Rev. B **45**, 9292 (1992).

[22] B. E. Warren, *X-ray diffraction* (Dover, New York, 1990).